

Europium-Doped ZnAl₂O₄ Nanophosphors: Structural and Luminescence Properties

A. Fernández-Osorio, C.E. Rivera, J. Chávez

Universidad Nacional Autónoma de México. México C.P.54740, Mexico
ana8485@unam.mx; claudiarivez@gmail.com

Abstract- Nanocrystalline zinc aluminate (ZnAl₂O₄) doped with Europium (III) solid solutions of ZnAl_{2-x}Eu_xO₄ (x=0, 0.01, 0.03, 0.06, 0.09 and 0.12) was synthesized by a chemical co-precipitation reaction from the corresponding metallic salts and subsequent calcination. Rietveld refinement of the X-ray powder diffraction (XRD) profile of the samples confirms the presence of the solid solution, with strong evidence that the europium ions substitute for the aluminum ions in the normal spinel structure. The crystallite average size of this system is 6.0±2.0 nm, as determined by XRD. The effects of europium concentration on the luminescence properties of the final materials were studied. The PL spectra exhibited a prominent and broader red emission band centered at 616 nm, corresponding to the ⁵D₀ → ⁷F₂ transition of octahedrally coordinated Eu³⁺ ions under an excitation wavelength of 260 nm.

Keywords: Nanophosphors; Solid solutions; Rietveld refinement; Luminescence properties.

1. Introduction

An enormous number of host/activator combinations have been studied for luminescence, with a fair degree of success. However, the development of new materials will most likely require an improved understanding of the relationship between the host crystal structure and the energy levels of the dopant ions. The crystal structure of the host material has a tremendous effect on the resulting emission intensity. Barghava et al. reported that the radiative transition rate of ZnS:Mn nanocrystals increased five-fold compared with that of the bulk.

Rare-earth ions are widely used as activators in different hosts due to their high fluorescence efficiencies when the size of their particles is reduced to the nanoscale; these materials are widely used in diverse applications, such as in fluorescent lamps, cathode-ray tubes, light-emitting diodes (LEDs) for the lighting industry, field-emission displays and X-ray imaging as shown by Ronda et al. (2008). Among these luminescent materials, Eu-activated phosphors have been studied intensely because Eu³⁺ is an ideal red-emitting activator, and Eu²⁺ can emit photons over a wide energy range, from UV to red, depending on the nature of the host as shown by Blasse et al. (1989).

ZnAl₂O₄ (ZA), is a semiconductor with an optical band gap of 3.8 eV, a representative material in the family of metal aluminates with a spinel structure, is widely used as a ceramic, electronic and catalytic material. Efforts have been devoted to studying the luminescent properties of pure and doped ZnAl₂O₄. Results have proved that ZnAl₂O₄ is a promising host with high efficiency and stability. Zinc aluminate has a normal spinel crystal structure with the space group Fd3m as shown by Sickafus et al. (1999). The coordination number of Al³⁺ in the octahedral sites indicates that it might be replaced by Eu³⁺; moreover, it is possible that the Eu³⁺ ions can be localized on the surface of ZnAl₂O₄ nanoparticles as shown by Silva et al. (2011).

To improve the luminescent properties of ZA:Eu³⁺ nanocrystalline phosphors, many preparation methods have been used, such as solid-state reactions, sol-gel techniques, chemical co-precipitation, hydrothermal synthesis, spray pyrolysis and combustion synthesis.

This work reports the structural and photoluminescence properties of Eu³⁺-doped ZnAl₂O₄ powders prepared by the co-precipitation method and subsequent calcination. Rietveld refinement based on

structure and microstructure as shown by Young et al. (1969), was adopted in the present analysis to determine several microstructural parameters as well as the occupation site of Eu^{3+} in doped ZnAl_2O_4 .

2. Material and Methods

The powder samples were characterized by X-ray diffraction (XRD), using a Siemens D5000 diffractometer with $\text{Cu K}\alpha$ radiation in the 2θ range of $2.5\text{-}70^\circ$.

The XRD data for Rietveld refinements were recorded in scan mode at 30 s/step and a step size of 0.05° over a 2θ range of $20\text{-}110^\circ$.

The refinement of structural parameters such as atomic coordinates, occupancies and lattice parameters and microstructural parameters such as particle size and lattice strain were obtained using the Rietveld method via the Fullprof 2003 Rietveld software.

Photoluminescence emission spectra were recorded at room temperature by a fluorescence spectrophotometer (F7000, Hitachi), with a 150-W xenon lamp as the excitation source.

2. 1. Experimental

Six samples were prepared according to the stoichiometry $\text{ZnAl}_{2-x}\text{Eu}_x\text{O}_4$ $x=0, 0.01, 0.03, 0.06, 0.09$ and 0.12 . All samples were synthesized by a co-precipitation reaction and subsequent calcination. First, stoichiometric amounts of the starting materials were dissolved in de-ionized water. In a typical synthesis, an aqueous solution of $\text{Zn}(\text{NO}_3)_2 \cdot 6\text{H}_2\text{O}$, $\text{AlCl}_3 \cdot 6\text{H}_2\text{O}$ and $\text{EuCl}_3 \cdot 6\text{H}_2\text{O}$ (all supplied by Sigma-Aldrich) was prepared. To this solution, 0.5 M ammonium hydroxide (NH_4OH) was added dropwise to obtain a precipitate composed of $\text{Zn}(\text{OH})_2$, $\text{Eu}(\text{OH})_3$ and $\text{Al}(\text{OH})_3$ at $\text{pH } 8 \pm 0.5$. The precipitate was washed twice with distilled water to remove Cl^- , NO_3^- and NH_4^+ ions, and the final product was dried at room temperature for one week. Subsequently, the powders were dried, ground and annealed in air at 900°C for 2 h.

3. Results and Discussion

3. 1. Crystal Structure

When the samples were annealed below 300°C , they were amorphous, and in the temperature range of $550\text{-}600^\circ\text{C}$, metal hydroxides crystallized into a nanocrystalline spinel structure. The powder X-ray diffraction patterns of un-doped ZnAl_2O_4 and Eu-doped ZnAl_2O_4 samples prepared by the co-precipitation method and heat treated at 900° for 2h are shown in Fig.1. All samples showed similar XRD patterns. No differences in crystallinity were observed in the zinc aluminate nanocrystal samples with various Eu doping concentrations. The XRD patterns of the samples revealed the formation of the ZnAl_2O_4 (gahnite) phase as a single phase in all of the sample compositions.

Fig. 2 shows the X-ray diffraction pattern of the sample $\text{ZnAl}_{1.94}\text{Eu}_{0.06}\text{O}_4$ sample annealed at 900°C . All reflections could be indexed to the spinel ZnAl_2O_4 phase (ICCD PDF-2 card 01-070-8183), with space group $\text{Fd}3\text{m}$ and cell parameter $a=8.059 \text{ \AA}$. A single phase was observed, indicating that homogeneous, Eu^{3+} -doped ZA solid solutions were formed. This sample presented an average crystallite size of 6.3 nm, determined by the classical Scherrer equation, using the broadening of the X-ray diffraction peaks over all reflections.

Note that Eu^{3+} ions are expected to occupy Al^{3+} sites in the ZnAl_2O_4 lattice, and because the ionic radius of Eu^{3+} is greater than that of Al^{3+} , the incorporation of the former will most likely strain the crystal lattice. Small crystallites lead to broad reflections, and variations in lattice spacing due to lattice strain cause diffraction peak broadening as shown by Warren et al. (1969).

The Rietveld refinement technique was used to determine the phase composition and verify the site occupation of Eu^{3+} in the spinel structure of the samples.

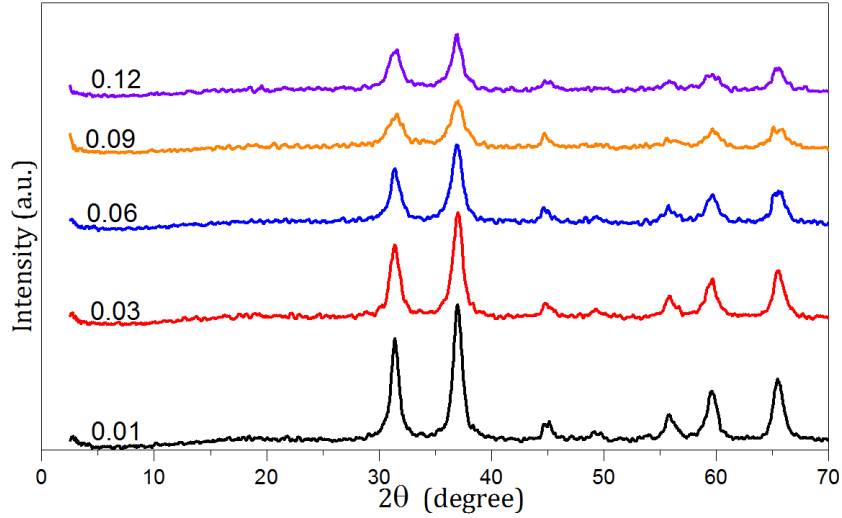


Fig. 1. X-ray diffraction patterns of $\text{ZnAl}_{2-x}\text{Eu}_x\text{O}_4$ ($x=0, 0.01, 0.03, 0.06, 0.09$ and 0.12)

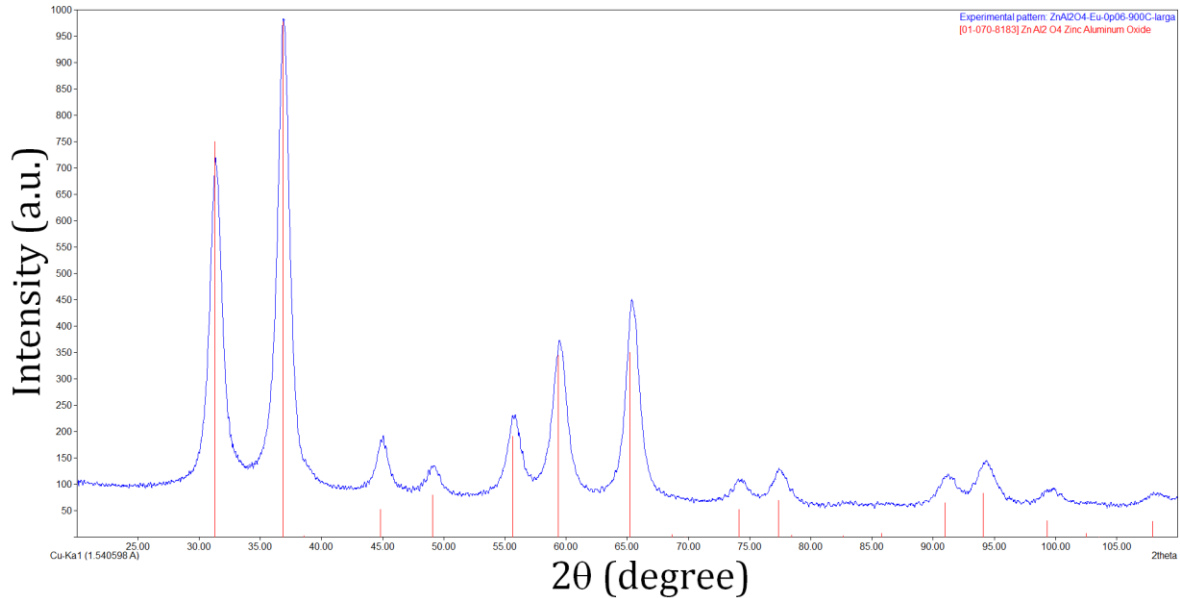


Fig. 2. X-ray diffraction pattern of $\text{ZnAl}_{1.94}\text{Eu}_{0.06}\text{O}_4$ sample annealed at 900°C

Rietveld refinement of the samples was carried out using one model based on a cation disorder model of the $\text{Fd}3\text{m}$ space group with cations filling the tetrahedral, 8a, and octahedral, 16d, sites, with a single oxygen site, 32e. Several constraints were applied at the start of the refinement. The thermal parameters were constrained to be the same for all atoms sharing a particular site, and the total occupancy of sites was set to unity. Broadening of the diffraction peaks was analyzed through the refinement of the regular TCH pseudo Voigt function parameters and the multipolar functions.

The calculations were performed for the $\text{Fd}3\text{m}$ space group in which the octahedral 16d sites are shared by Al^{3+} and Eu^{3+} ions and the tetrahedral crystallographic 8a sites are occupied by Zn^{2+} ions, which suggests a normal spinel structure. Eu^{3+} ions have an ionic radius of 95 pm, and Al^{3+} ions have an ionic radius of 54 pm as shown by Shannon et al. (1989). Due to their large ionic radius, the Eu^{3+} ions tend to prefer sites with high coordination numbers because in this spinel structure, the octahedral sites are occupied by Al^{3+} ions; in spite of the unusual size matching, these are the most likely sites to be replaced by Eu^{3+} . Fig. 3 presents a typical Rietveld refined X-ray pattern of the ZA:Eu 6 mol% sample.

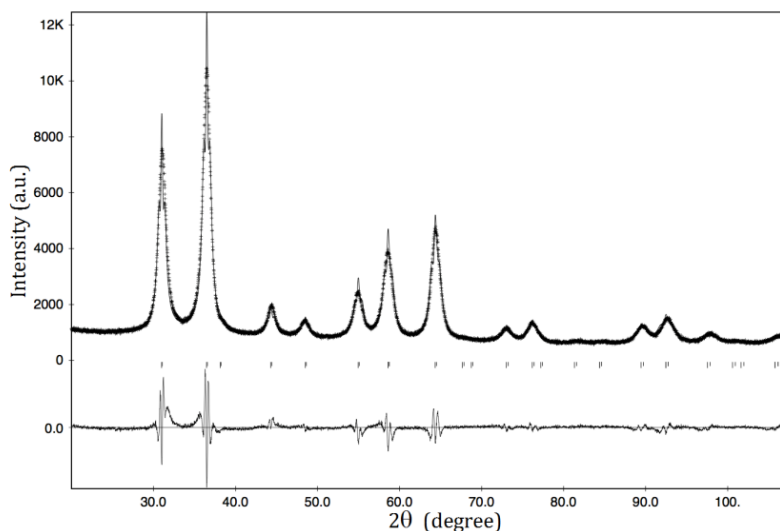


Fig. 3. Rietveld refinement of XRD pattern of $\text{ZnAl}_{1-x}\text{Eu}_x\text{O}_4$ ($x=0.03$) sample

The values of the discrepancy factor (R_{WP}), expected values (R_{EXP}) and Bragg values (R_{BRAGG}) and the structural information are summarized in Table 1.

Table. 1. Refined structural parameters for $\text{ZnAl}_{2-x}\text{Eu}_x\text{O}_4$ $x=0.03$.

| Atom | Wyckoff | Site Symmetry | x | y | z | B | N |
|-------------|---------|-----------------------|--------|-----------------|------------------|----------------|----------|
| Zn | 8a | 43m | 0.0000 | 0.0000 | 0.0000 | 0.2226 | 0.9953 |
| Al | 16d | 3m | 0.1250 | 0.1250 | 0.1250 | 0.0142 | 0.9699 |
| Eu | 16d | 3m | 0.1250 | 0.1250 | 0.1250 | 0.0142 | 0.0298 |
| O | 32e | 3m | 0.7375 | 0.7375 | 0.7375 | 0.0954 | 0.9978 |
| Space group | | Cell parameter, a (Å) | | R_{wp} | R_{exp} | R_{B} | χ^2 |
| Fd3m | | 8.2017 | | 8.41 | 6.49 | 2.75 | 1.29 |

The obtained R_{Bragg} indices confirm the high quality of the structure model. The refinement revealed that ZA:Eu is a normal spinel structure. It is clear from Table 1 that the lattice parameter increases with an increase in Eu^{3+} content, which can be explained based on the difference in the ionic radii between Al^{3+} (54 pm) and Eu^{3+} (95 pm). The resultant structure will present octahedral sites with a distorted geometry. Rietveld refinements also confirm the presence of Eu^{3+} ions in the octahedral sites. Some authors reported the appearance of additional sites of Eu^{3+} in nanocrystals due to the surface effect as shown by Streck et al. (2000). In the present case the ratio of surface to volume is high, but no additional sites were observed.

3. 2. Photoluminescence Properties

Fig. 10 shows the emission spectra of ZA samples doped with 0, 1, 3, 6, 9 and 12 mol% Eu under UV excitation (wavelength of 264 nm).

All spectra have two broader emission bands: one weak band located at 586 nm and an intense band located at 616 nm. The transition at 586 nm (${}^5\text{D}_0 \rightarrow {}^7\text{F}_1$) is a magnetic dipole transition, and the transition at 616 nm (${}^5\text{D}_0 \rightarrow {}^7\text{F}_2$) is an electric dipole transition as shown by Shinoya et al. (2006). As is well known, the ${}^5\text{D}_0 \rightarrow {}^7\text{F}_1$ band originated from a magnetic dipole transition, which hardly changes with the crystal field around Eu^{3+} , whereas the ${}^5\text{D}_0 \rightarrow {}^7\text{F}_2$ band originates from an electric dipole transition.

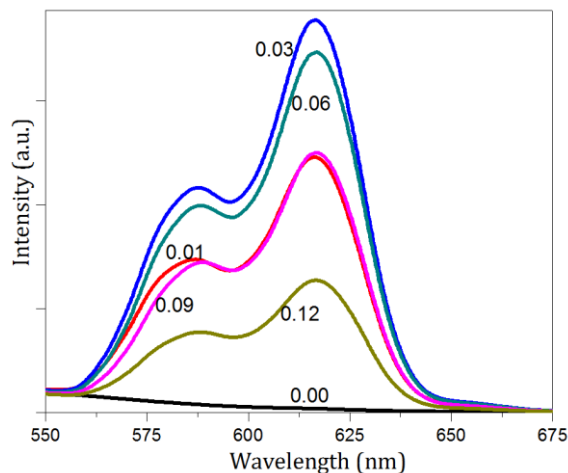


Fig. 4. PL spectra of $\text{ZnAl}_{2-x}\text{Eu}_x\text{O}_4$ ($x= 0, 0.01, 0.03, 0.06, 0.09$ and 0.12) under an excitation of 264 nm.

The magnetic dipole transition is permitted, the electric dipole transition is allowed only on the condition that the Eu^{3+} occupies a site without an inversion center and is sensitive to local symmetry. Subsequently, when Eu^{3+} ions occupy inversion center sites, the ${}^5\text{D}_0 \rightarrow {}^7\text{F}_1$ transition should be relatively strong, whereas the ${}^5\text{D}_0 \rightarrow {}^7\text{F}_2$ transition should be relatively weak. The results shown in the spectra (Fig. 9) indicate that Eu^{3+} ions occupy sites without an inversion center; thus, this transition is highly sensitive to structural changes in the vicinity of the Eu^{3+} ions. The asymmetric nature of the metal environmental arises from the fact that Eu^{3+} ions, after replacing the Al^{3+} ions, will occupy a highly distorted octahedral site due to the size mismatch but maintain their coordination number.

The maximum PL intensity was observed for ZA:Eu 3 mol% sample, corresponding to the composition $\text{ZnAl}_{1.97}\text{Eu}_{0.03}\text{O}_4$. Quenching concentration was observed at higher concentrations.

The quenching concentration of rare-earth ions is explained by the non-radiative energy transfer between activator ions, which occurs by interactions such as exchange interactions and multipole-multipole interactions as shown by Dexter et al. (1954).

4. Conclusion

$\text{ZnAl}_{2-x}\text{Eu}_x\text{O}_4$ ($x= 0, 0.01, 0.03, 0.06, 0.09$ and 0.12) nanoparticles with a single crystalline spinel phase were prepared by a co-precipitation method. Single-phase ZA:Eu³⁺ powders possessing particle sizes less than 10 nm were obtained at a processing temperature of 900°C. The average crystallite size diminished as the europium concentration increased. The TEM data showed that the particles were spherical in shape and that their average diameter was 7 ± 2.0 nm.

The Rietveld refinements of the ZA:Eu samples using X-ray diffraction data were successfully applied to determine the existence of the preferred sites of Eu^{3+} ions and the amount of Eu^{3+} ions in the octahedral sites in the spinel structure.

Among the samples synthesized, the maximum PL emission intensity was observed for the ZA:Eu 3 mol% sample, which showed a broad emission band at 616 nm under UV excitation (260 nm).

Acknowledgements

The authors wish to thank the CONACYT CB-2011/165539 project for financial support.

References

- Bhargava, N., & Gallagher, D. (1994). Optical Properties of Manganese-Doped Nanocrystals of ZnS. *Phys. Rev. Lett.*, 72, 416-419.
- Blasse, G., Grabmaier, B.C. (1994). *Luminescent Materials*. Berlin: Springer-Verlag.
- Dexter, DL., & Shulman, JH. (1954). Theory of Concentration Quenching in Inorganic Phosphores. *J. Chem. Phys.*, 22, 1063-70.

- Ronda, C. (2008). Luminescence. *From Theory to Applications* (1st. Ed.). Germany: Wiley-VCH.
- Shannon, R.D., & Prewitt, C.T. (1969). Effective Ionic Radii in Oxides and Fluorides. *Acta Crystallogr.*, *B25*, 925-946.
- Strek, W., Deren, P., Bednarkiewicz, A., Zawadzki, M., & Wrzyszczyk, J. (2000). Emission Properties of Nanostructured Eu Doped Zinc Aluminate Spinel. *J. Alloys. Compd.*, *300*, 456–458.
- Silva, D., Abreu, A., Davolos, M.R., & Rosaly, M. (2011). Determination of the Local Site Occupancy of Eu³⁺ ions in ZnAl₂O₄ Nanocrystalline Powders. *Opt. Mater.*, *33*, 1226-1233.
- Sickafus, K.E., Willis, J.M., & Grimes, N.W. (1999). Structure of Spinel. *J. Am. Cer. Soc.*, *82*, 3279 - 3292.
- Shinoya, S., Yen, W.M. (2006). *Phosphor Handbook*. Boca Raton, Florida: CRC Press.
- Warren, B.E. (1969). *X-ray Diffraction*. Addison-Wesley Pub. Co. Reading Mass.
- Young, R.A., & Wiles, D.B. (1969). Profile Shape Functions in Rietveld Refinements. *J. Appl. Crystallogr.*, *2*, 65-71.